Effect of Sintering Holding Time on the Corrosion Properties of Nano-Structured Fe-18Cr-2Si Alloy Prepared by SPS

Ihsan-ul-Haq Toor

Dept. of Mechanical Engineering, King Fahd University of Petroleum & Minerals (KFUPM)
Dhahran 31261, Kingdom of Saudi Arabia
E-mail: ihsan@kfupm.edu.sa, ihsan_jut@hotmail.com

Spark plasma sintering (SPS) was used to synthesize Nano-structured Fe-18Cr-2Si alloy with Fe-18Cr-2Si ball milled powders. SPS was carried out in vacuum at three different holding time (5, 10 and 15min) at a fixed sintering temperature (1100 °C) and applied pressure (50MPa). Potentiodynamic Polarization (PDP), Linear Polarization (LPR) and Electrochemical Impedance Spectroscopy (EIS) were used to study the effect of sintering time on the electrochemical properties of nanostructured alloy in deaerated 0.2M NaCl and 0.5M H_2SO_4 solutions respectively. Corrosion resistance measured in terms of corrosion potential (Ecorr), pitting potential (Epit) and passive current density (ip) was found to be increased with an increase in holding time. Density of the samples was measured by Archimedes' method and results showed the highest density for the specimen sintered for 15 min at 1100 ^{0}C.

1. INTRODUCTION

Stainless steel (SSs) production by powder metallurgy (PM) technique is of great importance because of the advantages for manufacturing bulk quantities of very small size, complex shaped components. In these days, it is of great importance to develop powder metallurgy SSs that can be exposed to high temperature applications (up to 800 ^{0}C, approximately). These PM SSs are used in turbo compressors, solid oxide fuel cells, parts of automotive exhausts (as exhaust flange and oxygen sensors boxes), etc. [1-5]. Although, the production of PM ferritic SSs are only a minor fraction of austenitic steels, the former are very important for certain applications [6]. Their low cost make them an optimum choice for mirror mounts in cars and the best choice for the manufacturing of antilock brakes system sensors because of their soft magnetic nature [1]. Good oxidation behavior make them

optimum choice for the applications in components used at high temperatures such as exhaust flanges, HEGO boxes, structural pieces of fuel cells, etc. [7, 8]. Conventional PM steels have intrinsically lower oxidation properties at high temperature in comparison with wrought fully dense steels with same compositions [9]. Studies showed that the porosity not only increases the effective area exposed to oxidation in many folds but also affects the nature of the protective film formed on the SSs [10]. Pore structure and morphology helps in the formation of poorly protective scales like pure or mixed iron oxides other than chromium oxide [11]. It has been reported as well that conventional PM SSs possess inferior corrosion properties than wrought steels [12-15]. The reason behind the inferior properties is not only the detrimental effects of pore structure/morphology but also the increase in effective surface area involved in corrosion. As corrosion rates are calculated by using apparent surface area but due to porosity, this factor increases to unknown folds [6].

The findings that, a nano-crystalline structure impart many distinctive properties to the materials [16] forced the researchers to prepare nano-crystalline SSs. A nano structure in PM SSs has been reported to impart high oxidation resistance [17]. The main reason for the improvement in oxidation properties is the diffusion of Cr and the ease of passive layer formation. It is believed that, the effect of nano structure on the corrosion behavior is dependent on the composition of the alloy and the severity of corrosion media [18]. SSs having nano crystalline structure will exhibit improvement in corrosion resistance in case of passivating electrolytes while undergo deterioration in the corrosion resistance in the presence of depassivating electrolytes [17]. The reasons for the improvement in corrosion properties in nano-crystalline SSs are because of the higher degree of Cr diffusivity, good compact passive layer and good adhesive nature of the passive layer. On the other hand, the degradation in corrosion resistance is because of the higher reactivity (owing to large no of grain boundaries) and residual stresses [18, 19]. Gupta et al. [18] investigated the corrosion performance of nanocrystalline and microcrystalline Fe20Cr alloys, prepared by high energy ball milling followed by compaction and sintering in acidic/ acidic chloride solutions. They found that the nanocrystalline alloy exhibited better corrosion resistance measured in terms of passivation potential, critical current density, passive current density and breakdown potential. The improved corrosion performance of these alloys was attributed to greater Cr content in the passive film formed on the nanocrystalline alloys. Garcia et al. [20] examined the corrosion performance of duplex stainless steels (DSSs) prepared by PM using 316L and 430L powders in hydrogen-nitrogen environment. They used different electrochemical techniques such as anodic polarization, cyclic anodic polarization scan and electrochemical potentio-kinetic reactivation test to determine the corrosion performance of these alloys. They found that when austenite/ferrite ratio was increased, the corrosion potential shifted to more noble values and passive current density was decreased. It was reported that DSS sintered in nitrogen cannot be used in as-sintered state due to their poor corrosion behavior, rather it should be used in solution annealed condition.

Though there have been few studies on ball milled Fe-Cr alloys, however there are not many studies reporting the effect of sintering time variation on the corrosion performance of spark plasma sintered, nanostructured Fe-Cr-Si alloys. So therefore, the objective of this study was to develop Fe-18Cr-2Si alloy by a combination of mechanical alloying (MA)/ SPS and to investigate the effect of sintering holding time variation on its corrosion performance. This study is a part of a comprehensive

work in which the independent effect of Si on the microstructure, mechanical and electrochemical properties of nano-structured ferritic Fe-18Cr-xSi(x=0~3) alloys is being investigated.

2. EXPERIMENTAL DETAILS

An in-house ball milled (Fe-18Cr-2Si) alloy powder with a crystallite size of 29.02 nm was used for sintering to make sintered pallets of 20 mm in diameter. FE-TEM investigation of milled powders showed a BCC crystalline structure in selected area diffraction pattern. A fully automated SPS machine (Type HP D-5, FCT Systeme, Rauenstein, Germany) was used for sintering the ball milled powders. Current was passed through a 20 mm graphite die, holding the powders. Samples were vacuum sintered and sintering temperature was measured with a thermocouple inserted in the graphite die through a drilled hole. To minimize the friction between die walls and powders, a graphite sheet was used, which also facilitates the specimen ejection after sintering.

Phase identifications after sintering were performed by using Bruker D8 advance equipped with Cu Kα radiation (λ=0.1542 nm). Morphological and microstructure investigations were performed by using JEOL FE-SEM. Archimedes' principle was employed to measure the density of sintered samples and a density determination kit supplied by METTLER Toledo was used for this purpose.

Corrosion tests were carried out in a three electrode cell, which composed of a specimen as a working electrode, a Pt wire as a counter electrode, and a saturated calomel reference electrode (SCE). The specimens were degreased in benzene, cleaned ultrasonically, and subsequently washed with distilled water prior to electrochemical tests. The investigations were carried out with an exposed working electrode area of 0.22 cm^2 in chloride (0.2M NaCl) and acidic (0.5M H2SO4) solution at room temperature in Gamry potentiostat (Reference 3000) and repeated thrice to ensure the reproducibility of the data. DC105 corrosion software was used to analyze the Tafel region, while Potentiodynamic polarization experiments were performed at a scan rate of 0.2mV/s. The specimens were cathodically cleaned -1.0 V$_{SCE}$ for 180 sec to remove any surface oxide scales before the anodic polarization scans. EIS tests were carried out by applying a sinusoidal voltage perturbation signal of 10 mV$_{SCE}$ with a frequency range of 100000Hz to 0.2Hz. Before EIS measurement, a stable passive film was formed potentiostatically for 30 minutes. Linear polarization resistance (LPR) tests were conducted by changing the potential from -0.02 to 0.02V$_{SCE}$ at a scan rate of 0.3mV/sec. The sample area was maintained to be 0.2cm^2. Before conducting the experiments, conditioning was done at -1 mV$_{SCE}$ for 3 min and 10-15 min were given for system stabilization. In order to calculate the polarization resistance (Rp), two points were selected on the straight data line and then Gamry software (DC105) was used for the calculations.

3. RESULTS & DISCUSSION

3.1. Phase Evolution of studies during milling and after sintering at three different holding times

Fig.1 shows the XRD spectra of Fe-18Cr-2Si alloy powder milled for 100 h as well as of sintered specimens of the same alloy at three different holding times. It is clear from Fig. 1 that

samples sintered at 5, 10, 15 min (at 1100 0C) showed the formation of α-ferrite phase after the sintering. The noise in the XRD of ball milled powders showed the strain in the powders due to ball milling. Peak broadening is an indications of refinement of powders. FE-TEM investigation and selected area diffraction pattern of milled powders confirmed the BCC crystalline BCC structure of starting powders as shown in Fig. 2.
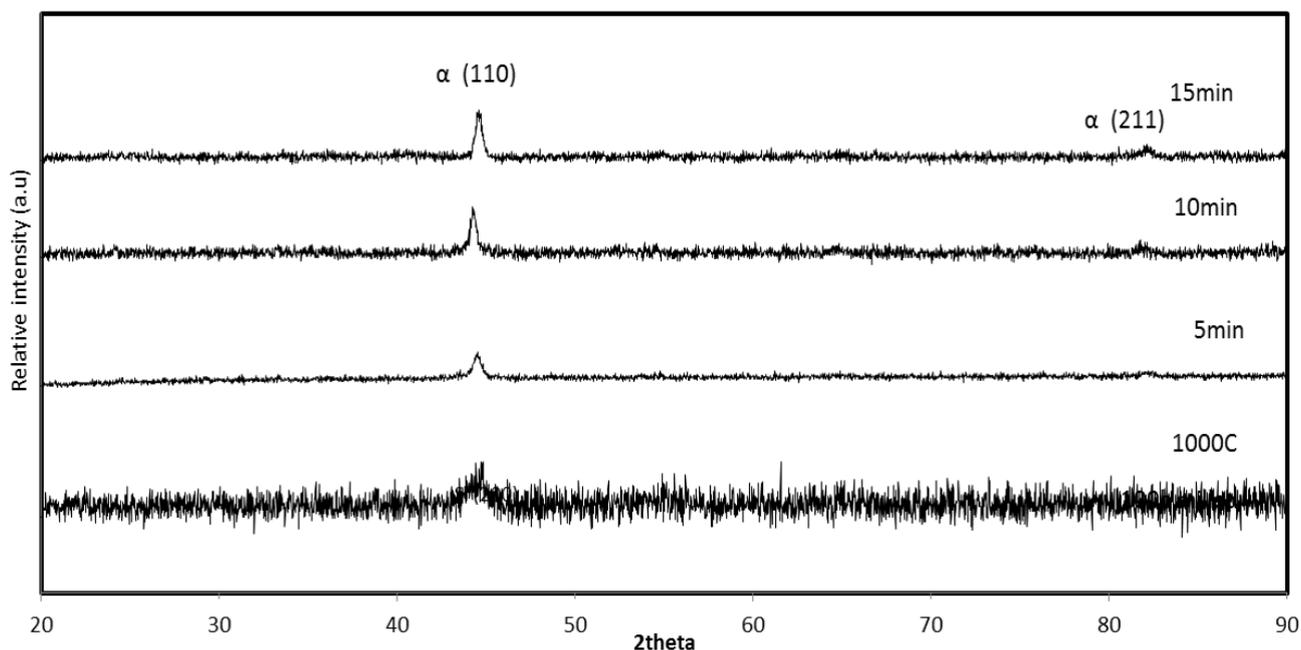

Figure 1. XRD patterns of spark plasma sintered Fe-18Cr-2Si powders at different sintering times, together with XRD spectra of 100 h milled powder.

Density calculation results showed an increase in densification with an increase in sintering time, mainly because of more given for sintering at a particular temperature (1100 ^{0}C). Densification was found to be 89.3%(at 5 min), 90.6% (10 min) and 91.4% (15 min) respectively. The increase in densification is directly related to the soundness of sintered alloys.

It was expected that the porosity of the alloy decreased substantially due to 15 min of holding at 1100 ^{0}C and contact among the powder particles was improved, which ultimately increased the densification. Micro hardness measurement revealed that, increase in sintering holding time resulted in an increase in hardness values.

Hardness was to be in the order of 680.5HV, 672.1HV, 653.3HV for specimens sintered at 15, 10 and 5 min respectively. FE-TEM investigation revealed the equiaxed structure with untextured BCC crystalline structure of Fe-18Cr-2Si alloys after sintering at three different holding times as shown in Fig.3.
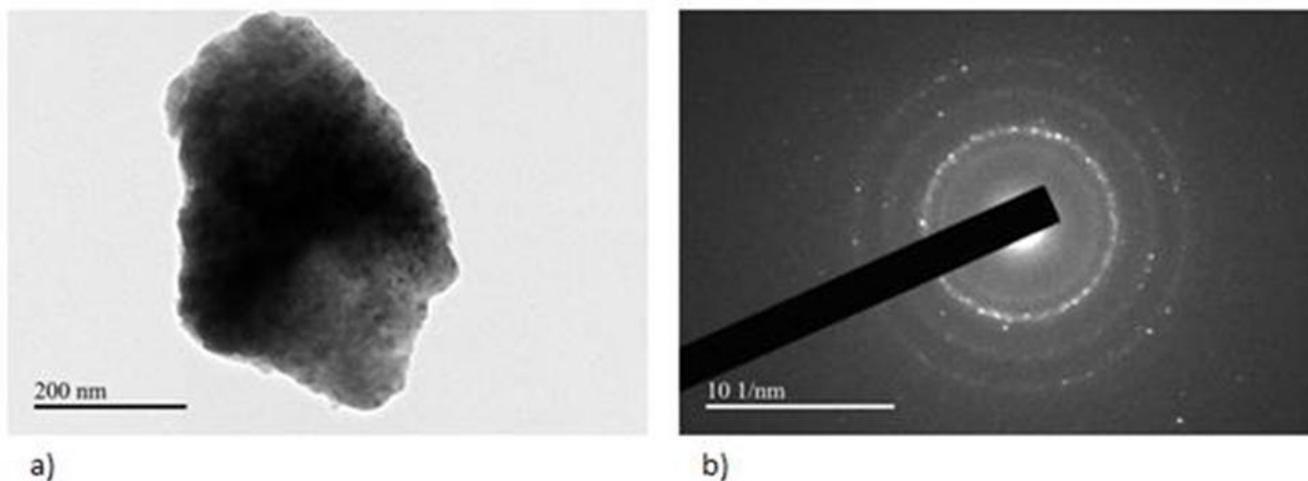
Figure 2. TEM bright-field images and selected area electron diffraction patterns of; (a) Fe-18Cr-2Si powder milled for 100 h (b) Micrograph of powder milled for 100 h showing the presence of BCC crystalline phase, confirmed from the diffraction pattern
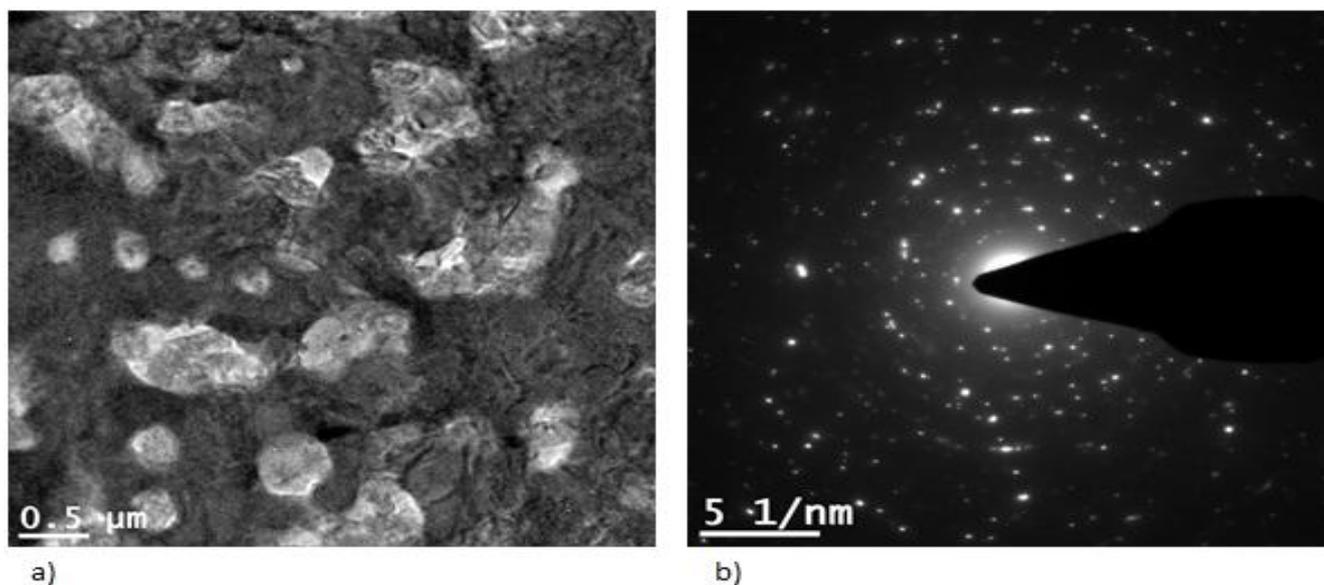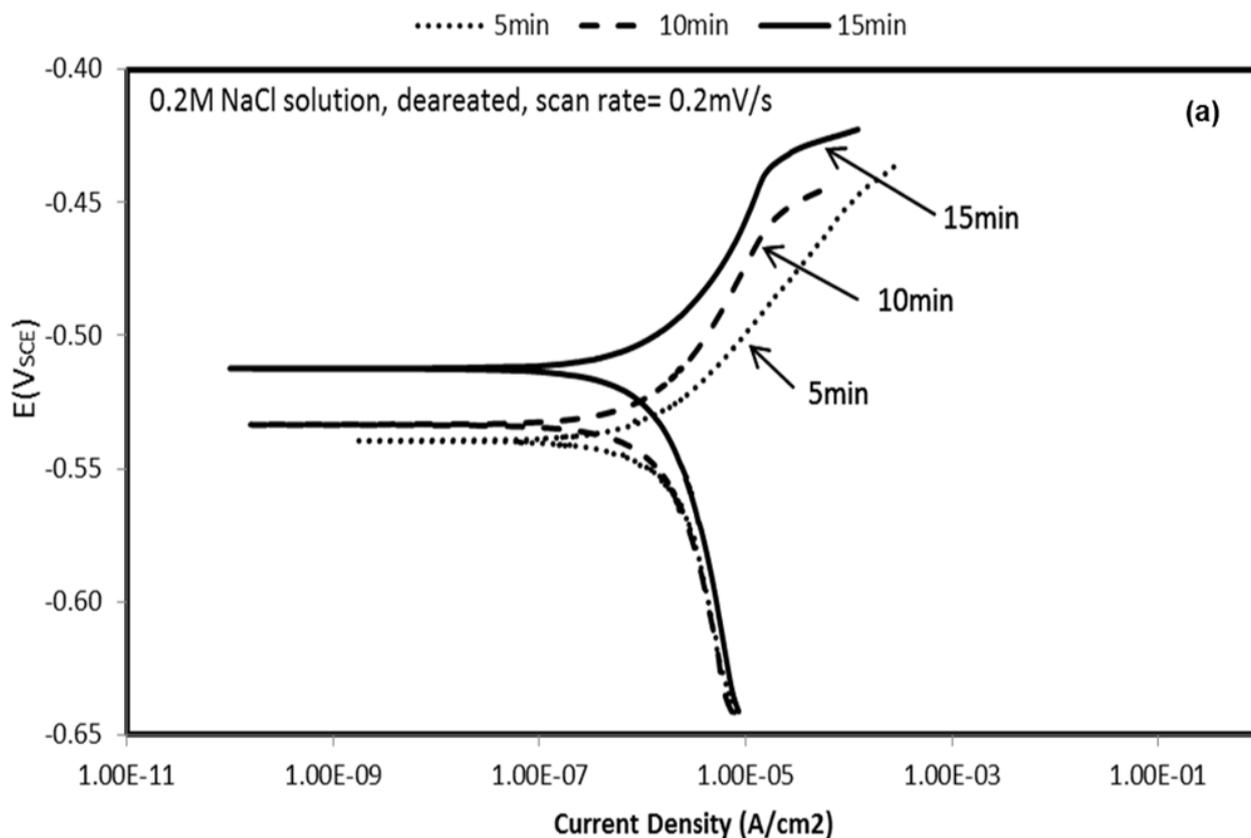

Figure 3.   Microstructure of Fe-18Cr-2Si sintered alloy (a)FE- TEM image, (b) SAED pattern

3.2. Effect of sintering time on the polarization response of the Fe-18Cr-2Si alloy

Fig. 4 (a) & (b) shows the potentiodynamic polarization response of Fe-18Cr-2Si alloy in 0.2M NaCl and 0.5M H2SO4 solutions at room temperature. Fe-18Cr-2Si alloy powder was sintered at three different holding times (5, 10, 15min) with a fixed sintering temperature of 1100°C at 50MPa applied pressure and 100 degree/min of heating rate. Based on densification and hardness experiments, it was found that the maximum densification and hardness was achieved with 15min holding time. So it was

expected that the specimen sintered at 15min will probably exhibit the highest corrosion resistance because of less porosity as compared to other two sintered specimens.

Guo et al. [21] has investigated the effect of density on the corrosion resistance of Ti-24Nb-4Zr-7.9Sn alloy and reported that alloys with lower density (sintered at low temperature) has lower corrosion resistance and vice versa. This lower corrosion resistance was due to more porous/less dense structure, when sintered at low temperature. When the density is high, it means the interconnected porosity is less, so there will be less chances of electrolyte penetration into such interconnected pores. On the other hand, lower porosity samples will have less corrosion resistance due to open interconnected porosity. It is very well known that porosity in sintered samples will allow the corrosion medium stagnation in pores, which will lead to crevice corrosion. So it is clear from Fig. 4 (a) & (b) that the specimen sintered with 15min holding exhibited the highest corrosion resistance in terms of pitting potential (Epit), passive current density (ip) and corrosion potential (Ecorr). The sample sintered at 1100°C for 15 min has an Epit value of -438.8 mV$_{SCE}$ and 234.2 mV$_{SCE}$ in 0.2M NaCl and 0.5M H$_2$SO$_4$ solutions respectively. Ecorr value was found to be -512.3 mV$_{SCE}$ and -340.1 mV$_{SCE}$ in 0.2M NaCl and 0.5M H$_2$SO$_4$ respectively. Fig. 4 shows that, the sample sintered with 5min of holding does not exhibit a stable passive film due to unstable passive film at low densification. The results of PDP tests are summarized in Table 1 and it is clear that specimen sintered at 1100 0C for 15 min has higher corrosion resistance.
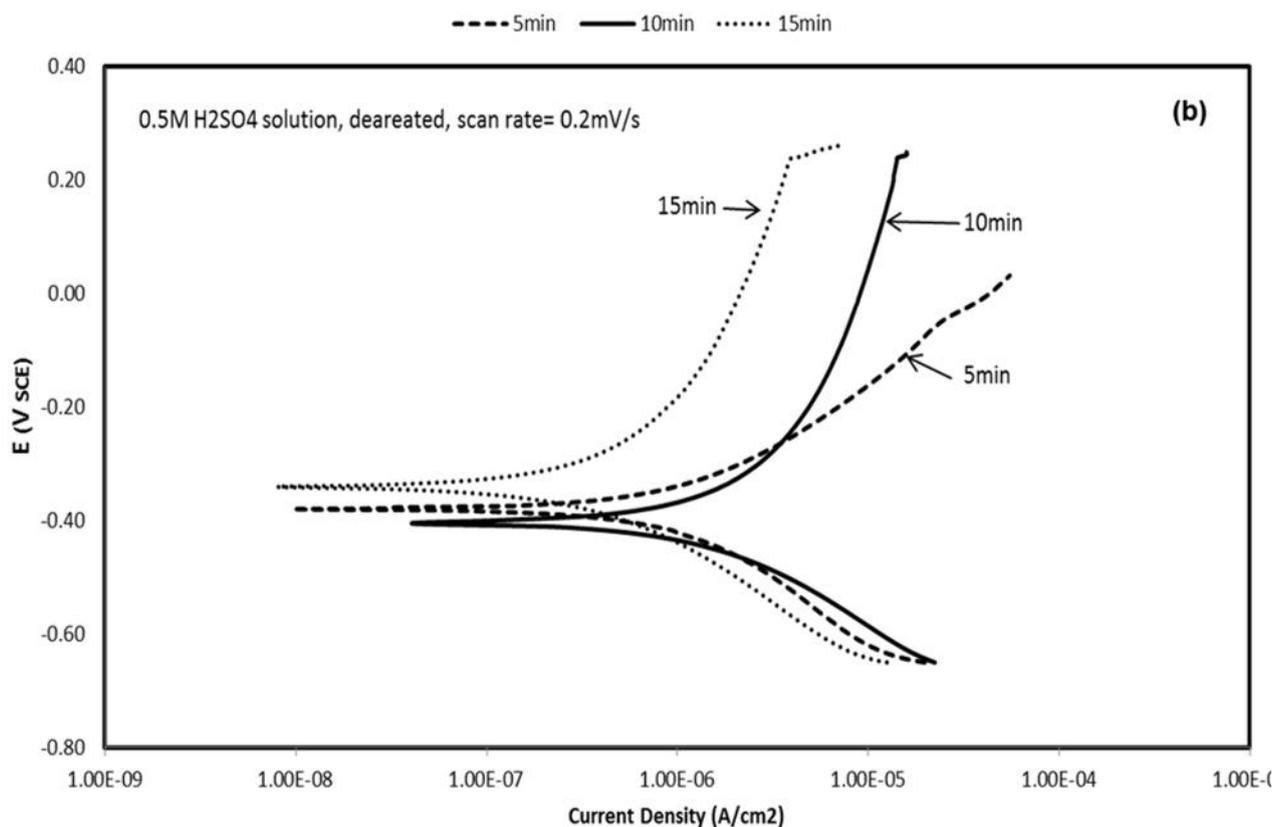
Figure 4. Potentiodynamic polarization response of Fe-18Cr-2Si specimens in deaerated, (a) 0.2M NaCl solution, and (b) 0.5M H_2SO_4 solution at room temp respectively.

A higher value of Ecorr means that the specimen (sintered at 15min) is nobler than rest of the specimens. Pitting potential (Epit), which is an important parameter for the investigation of localized corrosion resistance of passive materials is the highest for specimen sintered for 15 min which means it is the most resistant to localized corrosion under these conditions. Similarly the passive current density (ip) which is an important criterion to compare the passive metals was found to be the lowest for the specimen sintered for 15 min at 1100 ^0C, which means it has more stable and protective passive film and vice versa. Xie et al. [22] investigated the effect of pore characteristics on microstructure, mechanical properties and corrosion resistance of selective laser sintered porous Ti-Mo alloys and reported a lower corrosion resistance for high porosity samples.

Table 1. Summary of potentiodynamic polarization data of Fe-18Cr-2Si alloy sintered at three different holding times in 0.2M NaCl and 0.5M H2SO4 solutions respectively.

Sample#	0.2M NaCl				0.5M H2SO4			
	E_{corr} (mV_{SCE})	i_{corr} (nA)	E_{pit} (mV_{SCE})	i_p (μA)	E_{corr} (mV_{SCE})	i_{corr} (μA)	E_{pit} (mV_{SCE})	i_p (μA)
5min	-539.5	1.824	N/A	26.29	-378.3	31.23	-38.83	21.36
10 min	-533.4	0.1544	-460.1	8.474	-405	40.49	237.9	7.723
15 min	-512.3	0.548	-438.8	4.093	-340.1	8	234.2	1.88

The polarization resistance (Rp) is strongly dependent on the passive film formed on the surface of the specimen [23] and is the direct measure of the corrosion resistance of the material.

Fig. 5 (a) & (b) shows the polarization resistance of specimens sintered for 5, 10 and 15 min at 1100 ^{0}C in 0.2M NaCl and 0.5 M H2SO4 solutions respectively. Results showed that as the sintering holding time was increased, Rp value was increased in both solutions. Rp value of sample sintered at 1100˚C is much higher than that of samples sintered at 5 min and 10 min at same temperature. These results are agreement with potentiodynamic data discussed above. The specimen having the highest densification exhibited the best corrosion performance and that was the case here in Rp calculations as well. Gu et al. [24] investigated the corrosion performance of SSs coated Rebars and concluded that a process which gives dense coating (low porosity) presents high Rp values and vice versa. Thus the presence of pores/porosity (less dense) is the main reason behind low Rp values of specimens sintered for 5 and 10 min as compared to the one sintered for 15 min.
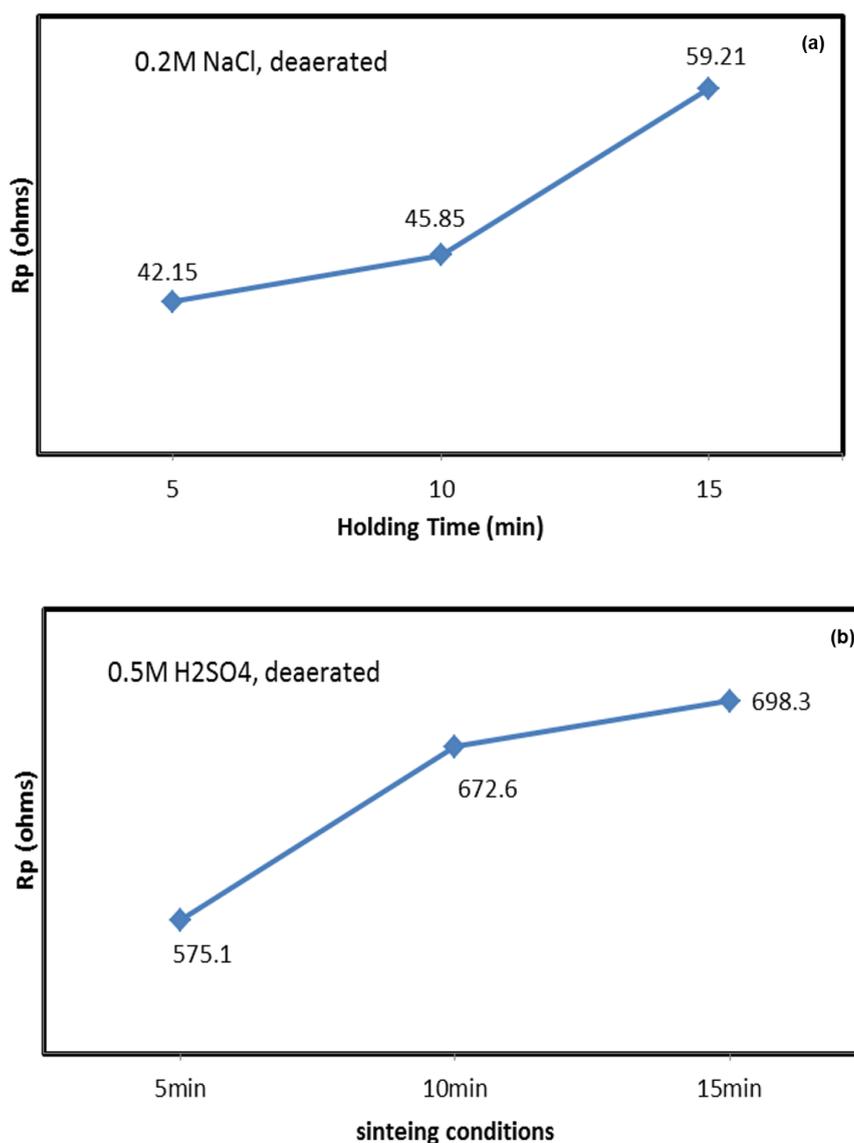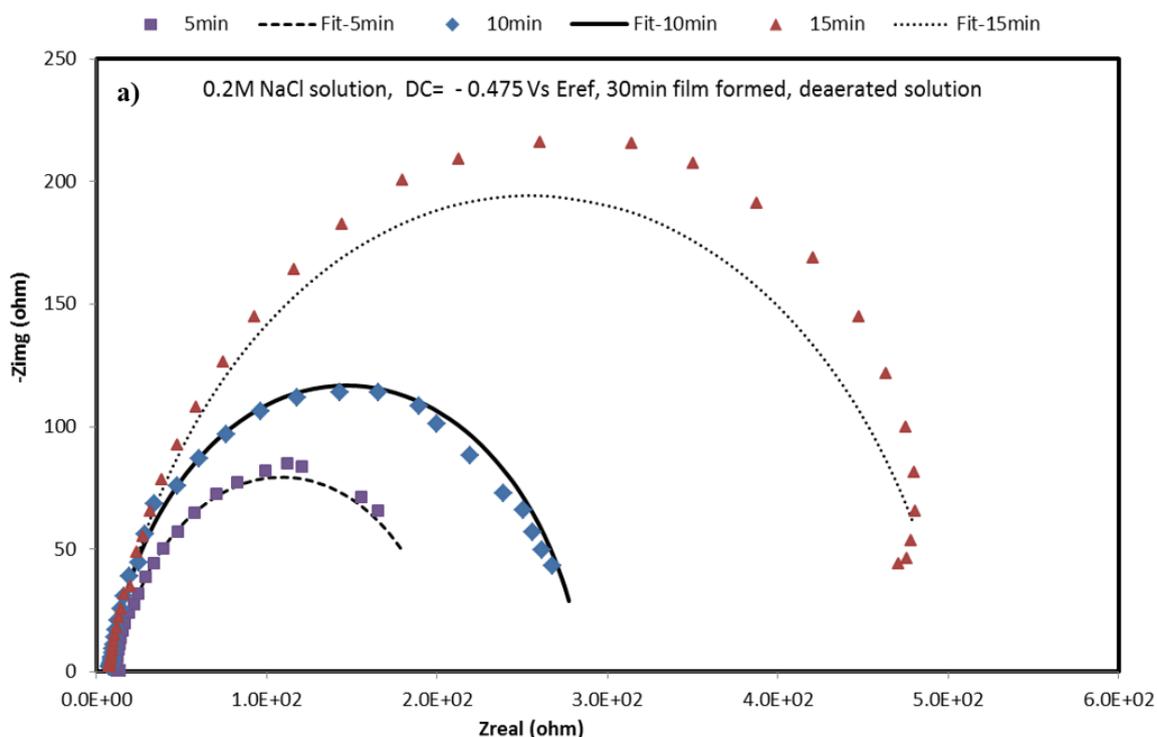

Figure 5. Polarization resistance (Rp) values versus time for Fe-18Cr-2Si specimens in deaerated, (a) 0.2M NaCl solution, and (b) 0.5M H2SO4 solution at room temp respectively.

3.3. Effect of sintering time on the impedance of the Fe-18Cr-2Si alloy

EIS response of sintered specimens was examined in chloride (0.2M NaCl) and acidic (0.5M H_2SO_4) solutions respectively. A potential in the passive range was selected (-0.47V$_{SCE}$ for NaCl & -0.20 V$_{SCE}$ for H2SO4 respectively) to carry out and the compare the EIS response of the samples sintered at different times. Before conducting the test, a passive film was formed for about 30 min.

Fig. 6 (a) & (b) shows the Nyquist spectra in both solutions. It is clear that the specimen sintered for 15 min has the highest spectra as compared to other two specimens. The diameter of the spectra is a direct function of the polarization resistance (Rp), which is inversely related to corrosion resistance, i.e. higher the value of Rp, lower will be the corrosion resistance. So therefore, it is concluded here that specimen sintered for 15 min at 1100 ^{0}C has highest corrosion resistance. Gu. et al. [24] reported that a coating with high porosity gave a complete semicircle with small diameter. On the other hand, the coating with low porosity exhibited an incomplete semicircle with large diameter. The coating having high porosity allowed the Cl$^-$ ions to pass and react with the substrate, which ultimately degraded the corrosion performance and resulted in lower value of Rp and vice versa. The results shown here exhibited that the specimens sintered for 5 min and 10 min has higher porosity/less densification as compared to 15 min specimen.

Since the EIS curves are relatively simple with only one time constant, the equivalent circuit shown in Fig.7 was used for quantitative study of the spectra and good quality fitting was obtained as shown in Fig. 6, together with the original data.
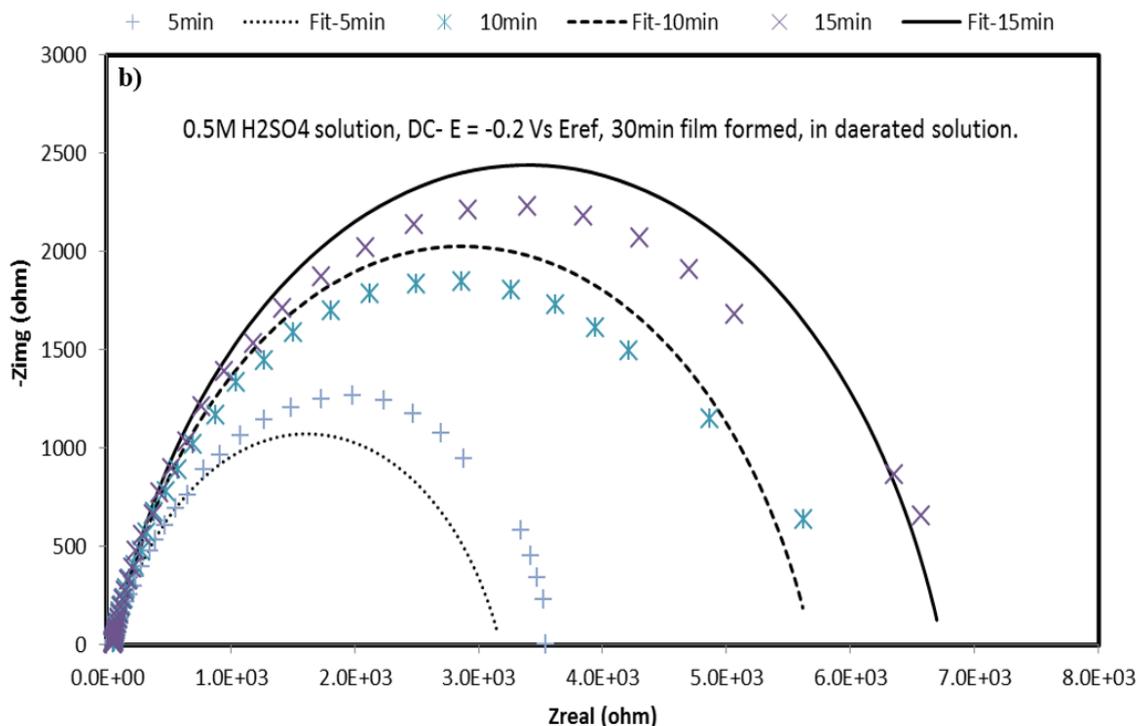
Figure 6. Nyquist plot of Fe-18Cr-2Si sintered specimens at different times together with CPE model curve fitting in deaerated (a) 0.2M NaCl solution, and (b) 0.5M H2SO4 solution at room temp., respectively.

The studies conducted on Fe-Cr alloy system reveals the double protective layer on the surface. This double layer consist of inner Cr-oxide layer which is actually in contact with the substrate and the outer layer contacted with electrolyte is of Fe-oxides and hydroxides. So, for EIS curve fitting, a double layer model was proposed as has been proposed previusoly by Bautista et al. [6]. In the equivalent circuit, a constant phase element "CPE" was used instead of capacitance because many times the measured capacitance is not ideal. The impedance representation of CPE is given by $Z(CPE) = 1/[Y_o(j\omega)^n]$ [23]. Here Y_o is the fit parameter. The physical meanings of the components involved in the circuit are as follows Rs correspond to the electrolyte resistance, CPE correspond to constant phase element and Rp is the polarization resistance of the passive film. Similar he same kind of model has been used by Wallinder et al. to study the effect of surface conditions on the corrosion of 316VM SSs [23]. The results obtained after EIS curve fitting are summarized in Table 2.
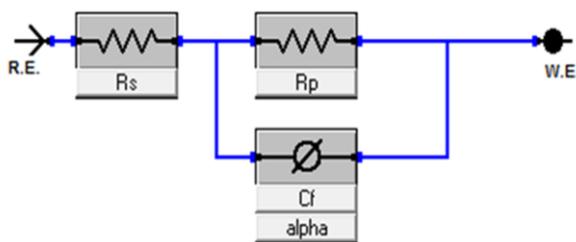

Figure 7. Constant phase element (CPE) model used to fit EIS data (Nyquist plot) in Figure 6

Table 2. Summary of the EIS curve fitting of Fe-18Cr-2Si alloy sintered at three different holding times in deaerated 0.2M NaCl and 0.5M H2SO4 solutions respectively

Sample#	0.2M NaCl		0.5M H2SO4	
	Rp(ohms)	Rs(ohms)	Rp(ohms)	Rs(ohms)
5min	240.6	7.315	3.13E3	51.74
10min	277.8	7.86	5.64E3	52.49
15min	533.3	7.428	6.69E3	51.82

4. CONCLUSIONS

A nano-crystalline Fe-18Cr-2Si ferritic alloy was prepared by a combination of MA and SPS. Results of sintering time variation at 1100 ^{0}C can be concluded as follows;

1- XRD and TEM of the specimens sintered for different times (5, 10, 15 min) at 1100 ^{0} confirmed the formation nanocrystalline alpha ferrite phase.

2- Corrosion resistance measured in terms of E_{pit}, E_{corr} and i_P was found to be the highest for the specimen sintered for 15 min at 1100 ^{0}C.

3- Polarization resistance (R^p) was found to be the highest for the specimen sintered for 15 min at 1100 ^{0}C.

4- Nyquist plots obtained in EIS confirmed that the specimen sintered for 15 min has highest corrosion resistance.

References

1. R.J. Causton, C. Mumau, T.M. Cimino, *Metal Powder Report*, 53 (2007) 22.
2. G.R. Romanoski, L.L. Snead, R.L. Klueh, D.T. Hoelzer, *Journal of Nuclear Materials*, 283-287 (2000) 642.
3. T. Kaito, T. Narita, S. Ukai, Y. Matsuda, *Journal of Nuclear Materials,* 329-333 (2004) 1388.
4. W.J. Quadakkers, J. Piron-Abellan, V. Shemet and L. Singheiser, *Materials at High Temperatures*, 20 (2003) 115.
5. I. Antepara, I. Villarreal, L.M. Rodríguez-Martínez, N. Lecanda, U. Castro and A. Laresgoiti, *Journal of Power Sources*, 51 (2005) 103.
6. A. Bautista, A. Gonzalez-Centeno, G. Blanco and S. Guzman, *Materials Characterization,* 59 (2008) 32.
7. P. Samal and J.Terrell, *Metal Powder Report,* 56 (2001) 28.

8. A. Bautista, F. Velasco, M. Campos, M.E. Rabanal and J.M. Torralba, *Oxidation of Metals*, 59 (2003) 373.
9. S. Lal, G.S. *Oxidation of Metals*, 32 (1989) 317.
10. A. González-Centeno, F. Velasco, A. Bautista and J.M. Torralba, *Materials Science Forum*, 426-432 (2003) 4355.
11. A. Bautista, C. Moral, F. Velasco, C. Simal and S. Guzman, *Journal of Materials Processing Technology*,189 (2007) 344.
12. E. Otero, A. Pardo, M. Utrilla, E. Saenz and J. Alvarez, *Corrosion Science*, 40 (1998) 1421.
13. E. Otero, A. Pardo, E. Sáenz, M.V. Utrilla and P. Hierro, *Corrosion Science*, 38 (1996) 1485.
14. T. Raghu, S.N. Malhotra, P. Ramakrishnan, *Corrosion*, 45 (1989) 698.
15. L. Fedrizzi, J. Crousier, P.L. Bonora and J.P. Crousier, *Werkstoffe Und Korrosion*, 42 (1991) 403.
16. H. Gleiter, *Progress in Material Science,* 33 (1989) 223.
17. R.K. Gupta and N. Birbilis, *Corrosion Science,* 92 (2015)1.
18. R.K. Gupta, R.K.S. Raman, C.C. Koch and B.S. Murty, *International Journal of Electrochemical Science,* 8 (2013) 6791.
19. L. a. Dobrzanski, Z. Brytan, M. Actis Grande and M. Rosso, *Journal of Material Processing Technology*, 191 (20073)161.
20. C. Garcia, F. Martin and Y. Blanco, *Corrosion Science*, 61 (2012) 45.
21. S. Guo, A. Chu, H. Wu, C. Cai and X. Qu, *Journal of Alloys and Compounds*, 597 (2014) 211.
22. F. Xie, X. He, S. Cao, M. Mei and X. Qu, *Electrochimica Acta*, 105 (2013) 121.
23. D. Wallinder, J. Pan, C. Leygraf and A.Delblanc-Bauer, *Corrosion Science,*41 (1998) 275.
24. P. Gu, B. Arsenault, J.. Beaudoin, J.-G. Legoux, B. Harvey and J. Fournier, *Cement and Concret Research*, 28 (1998) 321.